Asian Journal of Chemistry; Vol. 32, No. 12 (2020), 3203-3208

ASIAN JOURNAL OF CHEMISTRY

https://doi.org/10.14233/ajchem.2020.22842

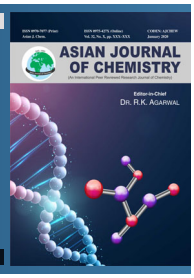

Curd Mediated Facile Synthesis of ZnO/Ag/NiO Heterostructures and Visible Light Assisted Photodegradation of Methylene Blue

J.P. SHUBHA[1,*], B.S. PRATHIBHA[2] and N. JAYALAKSHMI[3]

[1]Department of Chemistry, Don Bosco Institute of Technology (Affiliated to Visveswaraya Technological University, Belagavi), Kumbalagodu, Mysore Road, Bangalore-560074, India
[2]Department of Chemistry, BNM Institute of Technology (Affiliated to Visveswaraya Technological University, Belagavi), Bangalore-560070, India
[3]Department of Mechanical Engineering, University Visvesvaraya College of Engineering, Bangalore-560001, India

*Corresponding author: E-mail: shubhapranesh@gmail.com

Received: 27 May 2020; *Accepted*: 3 November 2020; *Published online*: 7 December 2020; AJC-20162

Green fuel perished curd was used to synthesize ZnO/Ag/NiO ternary heterostructure with zinc nitrate, nickel carbonate and silver nitrate as oxidizers. The obtained nanostructure was characterized by various analytical techniques such as powder X-ray diffraction (PXRD), Fourier transform infrared spectroscopy (FTIR), scanning electron microscopy (FESEM), transmission electron microscopy (TEM). The particles and flakes composition of ZnO/Ag/NiO nanomaterials was confirmed. Photocatalytic activity of ZnO/Ag/NiO was evaluated with methylene blue dye by source of light, concentration of hydrogen ion, catalyst and dye concentrations. The obtained ZnO/Ag/NiO nanoparticles reveal better catalytic property for the photodegradation of methylene blue dye under visible light.

Keywords: Curd, Heterostructures, Photocatalysis, Methylene blue.

INTRODUCTION

Dyeing is one of the major processes involved in weaving silk sarees (an Indian traditional attire) and other clothes. Dyeing centers located near to the unorganized weaving units. However, most of the hazardous dyes are disposed directly in open watercourses and drainages, causing a serious issue of water pollution in the surrounding the dyeing centers. Colour effluents are highly dangerous to living health [1]. Therefore, these problems are taken very seriously and currently handled by ecofriendly heterogeneous semiconductor photocatalysis methods [2-9].

Among all the photocatalysts ZnO [7,8], TiO_2 [10], CeO_2 [11,12] are widely used due to their suitable band gap energy. ZnO [7,8], TiO_2 [10], in their pure form and doped with inert metals like AgZnO [13-15], DyZnO [16], EuZnO [17-19], PtZnO [20], GdZnO [21], CuZnO [22], AuZnO [23], $AgCeO_2$ [24,25], $AgCu_2O$ [26], *etc*. are also used as photocatalysts. ZnO is active catalyst in UV light and it is incompetent under visible light so metal oxides such as Cu_2O [27], NiO [9], MnO_2 [28,29] are used under visible light. Further improvement is observed in clubbed metal oxides catalysts like ZnOCuO [30], ZnONiO [31-33], ZnOMnO [34], *etc*. under visible light. To enhance the photocatalytic activity of binary metal oxide composites, a metallic connection between them is used as ternary heterojunction [34-38]. Literature survey reveals that there are no reports on photocatalysis of ZnO/Ag/NiO. Therefore, the work is undertaken with the degradation studies of methylene blue.

EXPERIMENTAL

The chemicals *viz*. zinc nitrate hexahydrate, nickel carbonate and silver nitrate were of analytical grade and used without further purification. Methylene blue dye (SD fine chemicals, India) solution in distilled water was used as a model wastewater.

Different analytical tools like X-ray diffraction (Bruker diffractometer (CuKα (λ = 1.5406 Å) X-ray source), Fourier-transform infrared (Bruker IFS 66 v/S spectrometer) was used to characterize the samples. Surface morphology of the synthe-

sized material was studied by taking images with ZEISS Gemini SEM 500 microscope and structures were examined with transmission electron microscope (JEOL JEM2100 PLUS) operating at 200 kV accelerating voltage.

Synthesis of ZnO/Ag/NiO: Simple combustion method was used to synthesize ternary heterostructure ZnO/Ag/NiO nanoparticles. Stoichiometrically calculated amounts of zinc nitrate, nickel acetate and silver nitrate were thoroughly dissolved in 10 mL of distilled water and 6 mL perished curd under constant stirring for about 20 min. The solution was then taken to muffle furnace maintained at 400 ºC. A blackish powder obtained after 10 min was annealed for 3 h at the same temperature.

Photocatalytic activity: The activity studies were carried out by using ZnO/Ag/NiO nanoparticles as photocatalyst to regulate effective degradation of methylene blue under sunlight. An aliquot samples (5 mL) were withdrawn and their absorption was recorded. The change in the intensity of methylene blue (λ_{max} = 663 nm) is used to find percentage of decolorization.

In degradation experiment, 5, 10, 25 and 40 mg of ZnO/Ag/NiO was added to 100 mL of an aqueous solution of methylene blue at various concentrations *viz*. 5, 10, 15 and 20 ppm. Equilibrium attained between methylene blue and photocatalyst due to adsorption and desorption is achieved by keeping the aerated solutions in dark for about 30 min. At the time of irradiation of light, the aqueous mixture (4 mL) was collected at an interval of 30 min each from the reaction solution and the catalyst in the mixture was separated by centrifuging the mixture.

The degradation percentage of methylene blue dye can be determined by substituting initial (C_i) and final (C_f) dye concentrations as follows:

$$\text{Degradation } (\%) = \frac{(C_i - C_f)}{C_i} \times 100$$

RESULTS AND DISCUSSION

XRD studies: Fig. 1 shows the XRD patterns of ZnO, NiO and ZnO/Ag/NiO nanoparticles. All the diffraction peaks are crystallized in the mixed form of hexagonal and cubic structures of ZnO, NiO and Ag. Fig. 1b is the reference XRD pattern of ZnO obtained from ICSD which is hexagonal with the JCPDS no. 1-1136 and lattice parameters a = 3.242 Å and c = 5.176 Å while the space group is P63mc (no.186). Similarly, Fig. 1c show the powder diffraction pattern of NiO with cubic structures JCPDS no. 4-835 with lattice parameter a = 4.1769 Å with a space group $Fm\bar{3}m$ (no. 225) and cubic AgNPs are shown in Fig. 1d with JCPDS no. 4-783, lattice parameter a = 4.0862 and space group $Fm\bar{3}m$ (no. 225) taken as a reference from ICSD.

FTIR studies: The FTIR spectrum of ZnO/Ag/NiO nanoparticles was recorded in the range 4000-400 cm^{-1} (Fig. 2). The characteristic peaks 565 and 408 cm^{-1} are due to Zn-O and Ni-O stretching vibrations, respectively.

UV-Visible studies: Fig. 3 shows the UV-vis absorption spectrum of as-prepared ZnO/Ag/NiO. The spectrum shows the absorption range from 800 to 250 with maximum absorption

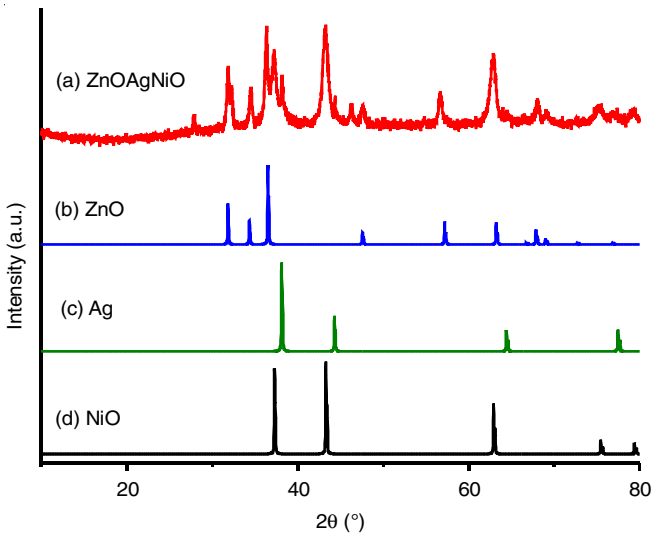

Fig. 1. XRD patterns of (a) ZnO/Ag/NiO composite, (b, c & d) ZnO, Ag and NiO reference

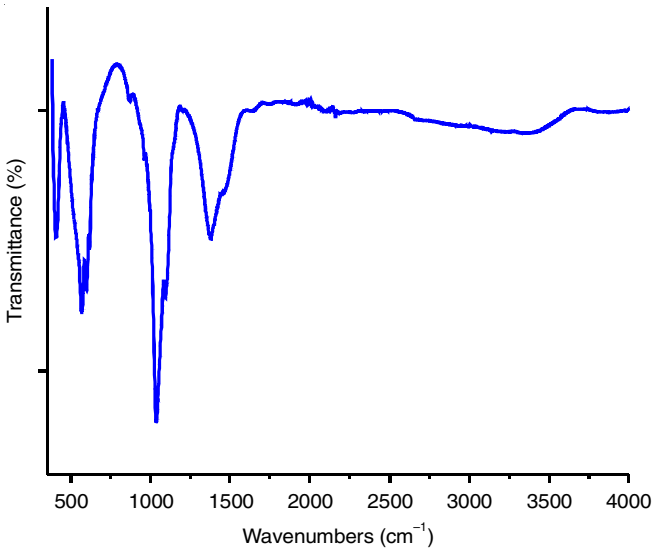

Fig. 2. FITR spectrum of ZnO/Ag/NiO

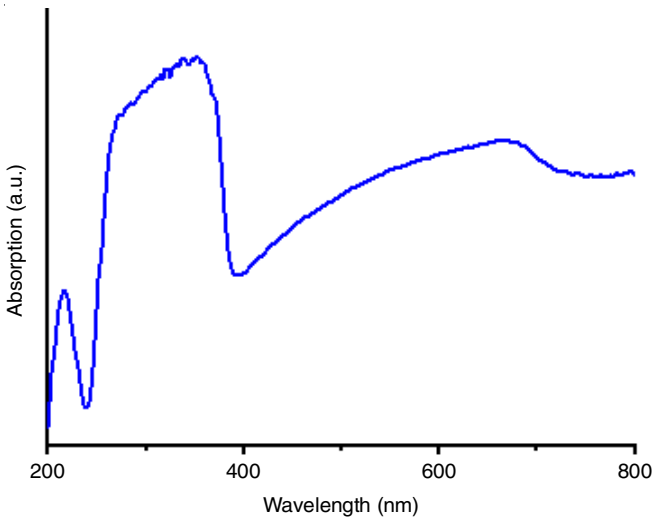

Fig. 3. UV-Vis spectrum of ZnO/Ag/NiO

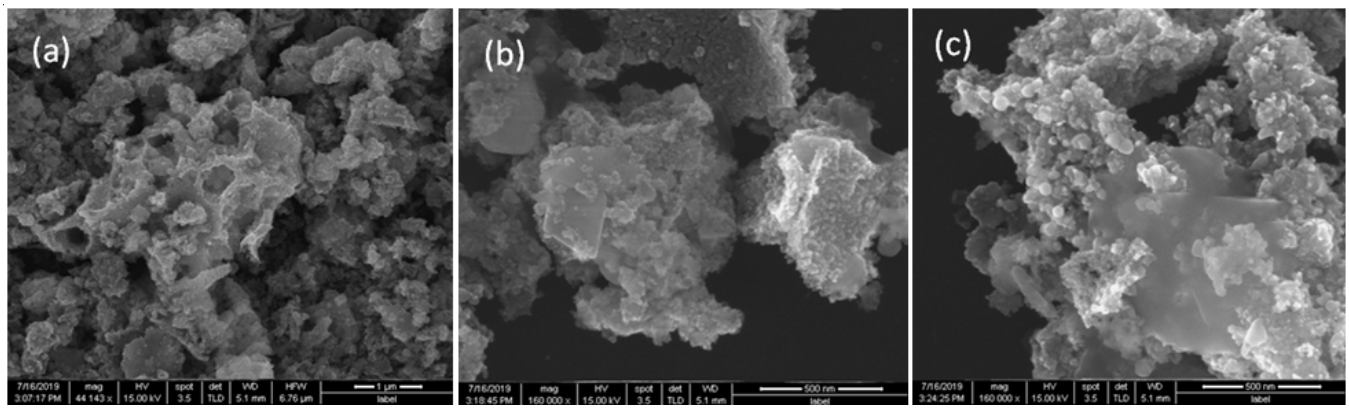

Fig. 4. FESEM images of ZnO/Ag/NiO with (a) Low magnification, (b) high magnification showing particles, (c) high magnification showing flakes

at 392 nm, which shows that ZnO/Ag/NiO is more compatible to absorb wide range of light both from UV and visible regions. Using Kulbeka-Munk equation, the band gap of the material is found to be 3.05 eV. Wide range of absorption of light helps in effective photocatalytic degradation and enhances the efficiency.

Morphologies studies: Fig. 4a depicts a low magnification FESEM image of ZnO/Ag/NiO, which indicated the particle and flake forms. High magnification FESEM image (Fig. 4b) shows the part of the material is in the form of flakes (like plate) in which all the particles are sprayed over it. Fig. 4c shows another part of high magnification image with spherical particles. It can be anticipated that ZnO and Ag are formed as particles and NiO formed as flakes.

Fig. 5a & b show the low and high magnification images, which demonstrates that the spherical particles are distributed all over the sample. The sizes of the particles are in the range between 20-50 nm. Fig. 5c represents the HRTEM image of ZnO/Ag/NiO, which indicates that lattice fringes width is about 0.24 nm and signifies the presence of silver nanoparticles belong to (111) reflection plane of Ag as also confirmed by XRD pattern. In addition, the selected area electron diffraction (SAED) pattern of the same compound (Fig. 6d) depicts that the material contains Ag which exists in polycrystalline nature and the reflection planes are corresponded with XRD pattern.

EDX studies: Fig. 6 shows the EDX spectrum of ZnO/Ag/NiO which designates that all the expected elements such as Zn, Ni, Ag, and O with other peaks are not nominated with any symbols (due to silica used for the sample preparation).

Effect of light source on photodegradation of methylene blue: All the experiments were carried out under sunlight. To ensure effective photocatalysis of ZnO/Ag/NiO NPs with sunlight, other light sources UV and dark conditions were also used to examine under similar experimental conditions. It is confirmed that photocatalyst ZnO/Ag/NiO is more efficient under sunlight (Fig. 7).

Effect of concentration of methylene blue on its photodegradation: To examine the effect of methylene blue concentration on its photodegradation with ZnO/Ag/NiO nanoparticles, dye concentration varied from 5 to 20 ppm by keeping other experimental variables like catalyst load and pH constant under

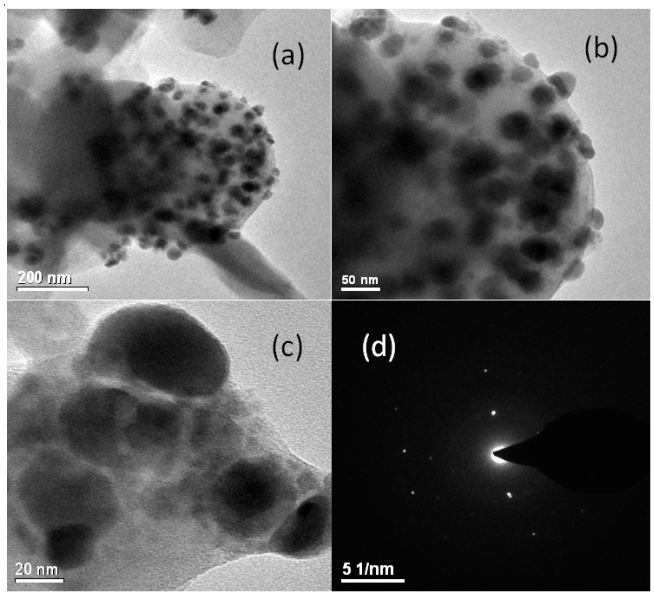

Fig. 5. TEM images of ZnO/Ag/NiO with (a) Low magnification, b) high magnification showing particles, c) HRTEM showing lattice fringes, and d) electron diffraction image

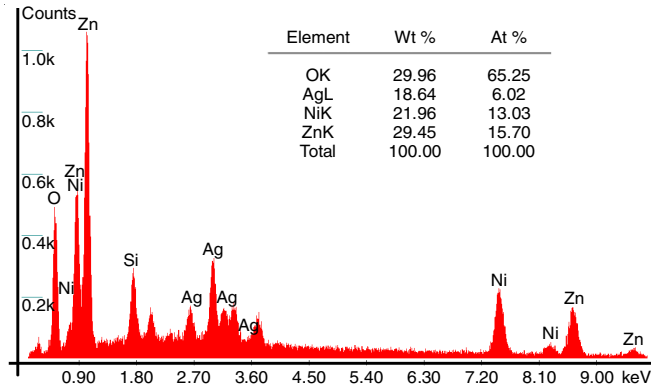

Fig. 6. EDX spectrum of ZnO/Ag/NiO with elements and its composition (inset Table)

solar light. The results revealed that the increased concentration of dye required appropriate increment in catalyst load which means increased dye decreased degradation. Since experiments were performed between 5 to 20 ppm under solar light, degra-

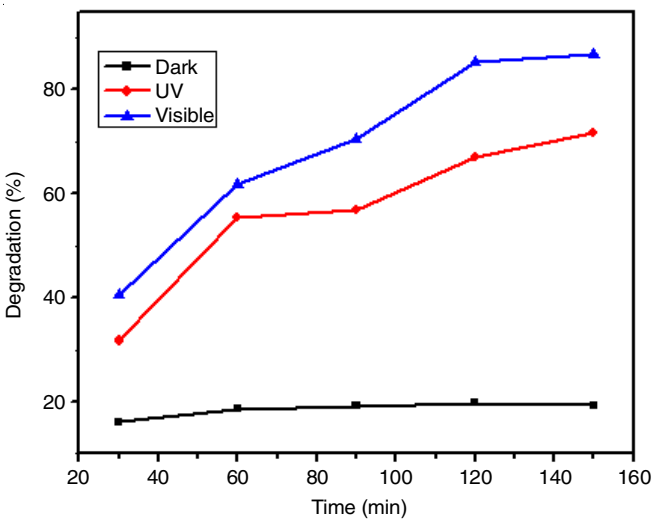

Fig. 7. Variation of light source on the degradation of methylene blue

dation of methylene blue decreased from 92% to 25% (Fig. 8). This may be due to decreased absorption of light on the surface of photocatalyst with increased dye concentration.

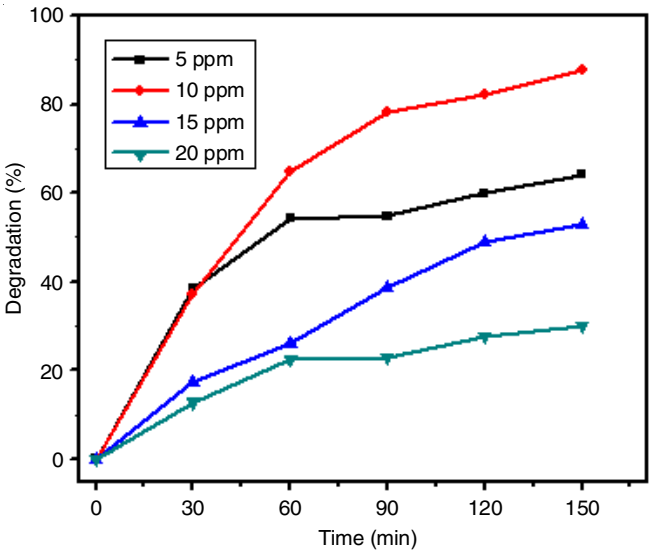

Fig. 8. Effect of dye concentration on the degradation of methylene blue

Effect of catalyst load: In general, a catalyst is used to alter the rate of reaction. Same way photocatalyst also increased the degradation of methylene blue which is demonstrated by varying the catalyst load from 5-40 mg while kept other parameters optimized. It was confirmed that degradation of methylene blue dye increased from 52% to 95% with increased load of photocatalyst 5-40 mg (Fig. 9).

Effect of pH: As photocatalytic efficiency of a photocatalyst is directly related to availability of hydroxyl radicals in the solution which is confirmed that rate of photocatalysis is usually more in alkaline solutions. In lower pH, degradation capacity of photocatalyst depends only on the rate generated hydroxyl radicals. This was demonstrated by varying the pH of a solution from 4-10 by keeping other parameters constant. Fig. 10 shows that degradation of methylene blue is fast at higher pH. Reaction conditions below pH 3 affect rate of degradation

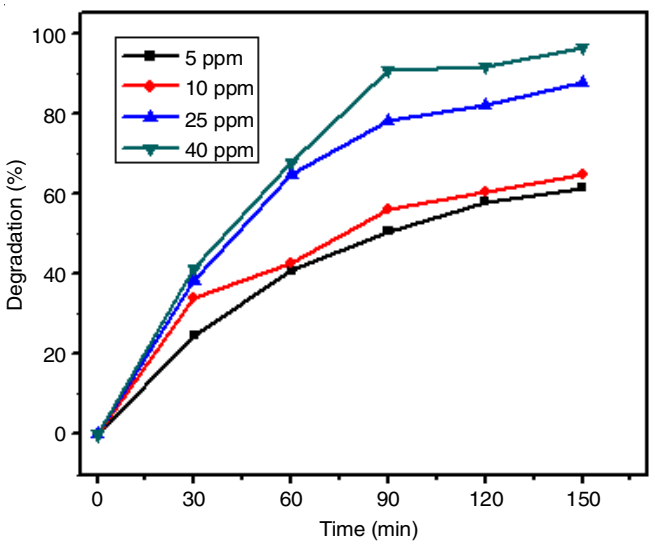

Fig. 9. Effect of catalyst load on the degradation of methylene blue

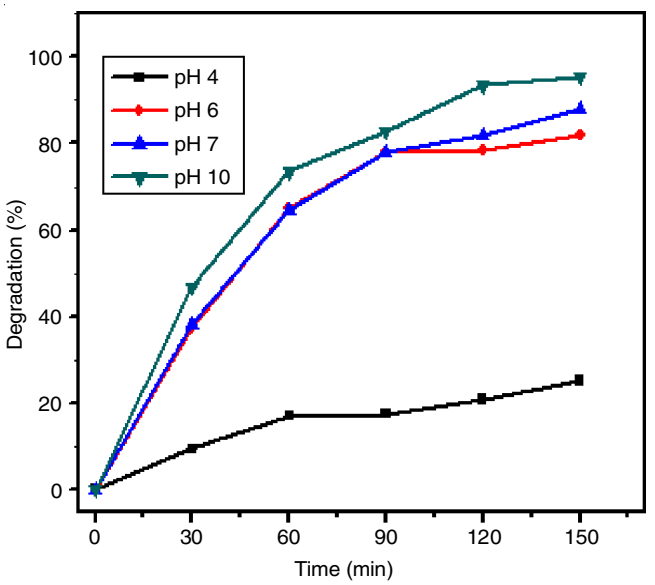

Fig. 10. Effect of [H^+] on the degradation of methylene blue

and above pH 8 ceases degradation of methylene blue. This is due to accumulation of hydroxyl radicals on the surface of catalyst.

Comparison of degradation efficiency of different nanocomposite: The photocatalytic degradation efficiency of ZnO/Ag/NiO is also compared with few other reported metal oxide nanocomposite against methylene blue dye (Table-1). It is observed that synthesized ternary heterostructure ZnO/Ag/NiO nanoparticles exhibit similar best degradation efficiency as compared to other reported materials.

Conclusion

In summary, waste curd is used as fuel to synthesize ternary heterojunction ZnO/Ag/NiO by combustion route. The prepared material showed enhanced photocatalytic activity towards methylene blue degradation under visible light illumination compared to their conventional materials reported in the literature.

TABLE-1
A COMPARISON WITH THE LITERATURE FOR DECOLORIZATION OF METHYLENE BLUE DYE

Material used	Light source	Catalyst load	Degradation time (min)	Degradation (%)	Ref.
WO_3/TiO_2	Visible light	5 mol%	120	52	[38]
$ZnO/NiFe_2O_4$	UV light	75 mg/50 mL	70	98	[39]
Bi_2WO_6/ZnO	Visible light	50 mg/100 mL	120	90	[40]
ZnO-NiO-Ag	UV light	20 mg/10 mL	90	94	[41]
ZnO/Ag/NiO	Visible light	40 mg/100 mL	150	97	Present work

ACKNOWLEDGEMENTS

The authors are thankful to VGST (SMYSR-2016; GRD 506), Government of Karnataka for the financial support and The Principal & Management, Don Bosco Institute of Technology for their support. Microscopy facilities provided by Technical Research Centre-Microscopy laboratory at JNCASR, Bangaluru, India are also gratefully acknowledged.

CONFLICT OF INTEREST

The authors declare that there is no conflict of interests regarding the publication of this article.

REFERENCES

1. H. Zollinger, Color Chemistry: Synthesis, Properties and Applications of Organic Dyes and Pigments, Wiley-VCH, Cambridge, edn 3 (2003).
2. K. Manjunath, T.N. Ravishankar, D. Kumar, K.P. Priyanka, T. Varghese, H.R. Naika, H. Nagabhushana, S.C. Sharma, T. Ramakrishnappa, J. Dupont and G. Nagaraju, *Mater. Res. Bull.*, **57**, 325 (2014); https://doi.org/10.1016/j.materresbull.2014.06.010
3. D. Suresh, P.C. Nethravathi, Udayabhanu, H. Rajanaika, H. Nagabhushana and S.C. Sharma, *Mater. Sci. Semiconductor Proc.*, **31**, 446 (2015); https://doi.org/10.1016/j.mssp.2014.12.023
4. H.R. Madan, S.C. Sharma, Udayabhanu, D. Suresh, H. Nagabhushana, Y.S. Vidya, H. Rajanaik, K.S. Anantharaju, S.C. Prashantha and P.S. Maiya, *Spectrochim. Acta A Mol. Biomol. Spectrosc.*, **152**, 404, (2016); https://doi.org/10.1016/j.saa.2015.07.067
5. P. Dash, A. Manna, N.C. Mishra and S. Varma, *Physica E*, **107**, 38 (2019); https://doi.org/10.1016/j.physe.2018.11.007
6. A.P. Shah, S. Jain, V.J. Mokale and N.G. Shimpi, *J. Ind. Eng. Chem.*, **77**, 154 (2019); https://doi.org/10.1016/j.jiec.2019.04.030
7. T. Khalafi, F. Buazar and K. Ghanemi, *Sci. Rep.*, **9**, 6866 (2019); https://doi.org/10.1038/s41598-019-43368-3
8. N.S. Pavithra, K. Lingaraju, G.K. Raghu and G. Nagaraju, *Spectrochim. Acta A: Mol. Biomol. Spectrosc.*, **185**, 11 (2017); https://doi.org/10.1016/j.saa.2017.05.032
9. A.K.H. Bashir, L.C. Razanamahandry, A.C.Nwanya, K. Kaviyarasu, W.Saban, S.K.O. Ntwampe, F.I. Ezema and M. Maaza, *J. Phys. Chem. Sol.*, **134**, 133 (2019); https://doi.org/10.1016/j.jpcs.2019.05.048
10. G. Nagaraju, K. Manjunath, T.N. Ravishankar, B.S. Ravikumar, H. Nagabhushan, G. Ebeling and J. Dupont, *J. Mater. Sci.*, **48**, 8420 (2013); https://doi.org/10.1007/s10853-013-7654-5
11. D. Channei, B. Inceesungvorn, N. Wetchakun, S. Ukritnukun, A. Nattestad, J. Chen and S. Phanichphant, *Sci. Rep.*, **4**, 5757 (2014); https://doi.org/10.1038/srep05757
12. P.K. Sane, S. Tambat, S. Sontakke and P. Nemade, *J. Environ. Chem. Eng.*, **6**, 4476 (2018); https://doi.org/10.1016/j.jece.2018.06.046
13. A. Phuruangrat, S. Siri, P. Wadbua, S. Thongtem and T. Thongtem, *J. Phys. Chem.*, **126**, 170 (2019); https://doi.org/10.1016/j.jpcs.2018.11.007
14. T.K. Pathak, R.E. Kroon and H.C. Swart, *Vacuum*, **157**, 508 (2018); https://doi.org/10.1016/j.vacuum.2018.09.020
15. Udayabhanu, G. Nagaraju, H. Nagabhushana, D. Suresh, C. Anupama, G.K. Raghu and S.C. Sharma, *Ceram. Int.*, **43**, 11656 (2017); https://doi.org/10.1016/j.ceramint.2017.05.351
16. A. Khataee, R.D.C. Soltani, Y. Hanifehpour, M. Safarpour, H.G. Ranjbar and S.W. Joo, *Ind. Eng. Chem. Res.*, **53**, 1924 (2014); https://doi.org/10.1021/ie402743u
17. M.A. Hernández-Carrillo, R. Torres-Ricárdez, M.F. García-Mendoza, E. Ramírez-Morales, L. Rojas-Blanco, L.L. Díaz-Flores, G.E. Sepúlveda-Palacios, F. Paraguay-Delgado and G. Pérez-Hernández, *Catal. Today*, **349**, 191 (2018); https://doi.org/10.1016/j.cattod.2018.04.060
18. D. Dash, N.R. Panda and D. Sahu, *Applied Surf. Sci.*, **494**, 666 (2019); https://doi.org/10.1016/j.apsusc.2019.07.089
19. Y. Zong, Z. Li, X. Wang, J. Ma and Y. Men, *Ceram. Int.*, **40**, 10375 (2014); https://doi.org/10.1016/j.ceramint.2014.02.123
20. M. Zayed, A.M. Ahmed and M. Shaban, *Int. J. Hydrogen Energy*, **44**, 17630 (2019); https://doi.org/10.1016/j.ijhydene.2019.05.117
21. S. Selvaraj, M.K. Mohan, M. Navaneethan, C. Muthamizhchelvan and S. Ponnusamy, *Mater. Sci. Semiconduct. Proc.*, **103**, 104622 (2019); https://doi.org/10.1016/j.mssp.2019.104622
22. N.T. Hanh, N.L.M. Tri, D.V. Thuan, M.H.T. Tung, T.-D. Pham, T.D. Minh, H.T. Trang, M.T. Binh and M.V.Nguyen, *J. Photochem. Photobiol. A: Chem.*, **382**, 111923 (2019); https://doi.org/10.1016/j.jphotochem.2019.111923
23. V. Vaiano, C. Augusto, M. Matarangolo, J. Antonio and M.C. Hidalgo, *Mater. Res. Bull.*, **112**, 251 (2019); https://doi.org/10.1016/j.materresbull.2018.12.034
24. K. Negi, A. Umar, M.S. Chauhan and M.S. Akhtar, *Ceram. Int.*, **45**, 20509 (2019); https://doi.org/10.1016/j.ceramint.2019.07.030
25. P. Verma, Y. Kuwahara, K. Mori and H. Yamashita, *Catal. Today*, **324**, 83 (2019); https://doi.org/10.1016/j.cattod.2018.06.051
26. Y. Sun, L. Cai, X. Liu, Z. Cui and P. Rao, *J. Phys. Chem. Solids*, **111**, 75 (2017); https://doi.org/10.1016/j.jpcs.2017.07.018
27. H. Manisha, P.D. Priya Swetha, Y.-B. Shim and K.S. Prasad, *Mater. Today Proc.*, **5**, 16390 (2018); https://doi.org/10.1016/j.matpr.2018.05.135
28. A. Gagrani, J. Zhou and T. Tsuzuki, *Ceram. Int.*, **44**, 4694 (2018); https://doi.org/10.1016/j.ceramint.2017.12.050
29. L. Xiao, W. Sun, X. Zhou, Z. Cai and F. Hu, *Vacuum*, **156**, 291 (2018); https://doi.org/10.1016/j.vacuum.2018.07.045
30. P. Bharathi, S. Harish, J. Archana, M. Navaneethan, S. Ponnusamy, C. Muthamizhchelvan, M. Shimomura and Y. Hayakawa, *Appl. Surf. Sci.*, **484**, 884 (2019); https://doi.org/10.1016/j.apsusc.2019.03.131
31. S. Chu, H. Li, Y. Wang, Q. Ma, H. Li, Q. Zhang and P. Yang, *Mater. Lett.*, **252**, 219 (2019); https://doi.org/10.1016/j.matlet.2019.05.145
32. Y. Liu, G. Li, R. Mi, C. Deng and P. Gao, *Sens. Actuators B Chem.*, **191**, 537 (2014); https://doi.org/10.1016/j.snb.2013.10.068
33. B.L. Martínez-Vargas, M. Cruz-Ramírez, J.A. Díaz-Real, J.L. Rodríguez-López, F.J. Bacame-Valenzuela, R. Ortega-Borges, Y. Reyes-Vidal and L. Ortiz-Frade, *J. Photochem. Photobiol. Chem.*, **369**, 85 (2019); https://doi.org/10.1016/j.jphotochem.2018.10.010

34. Z. Xiu, Y. Cao, Z. Xing, T. Zhao, Z. Li and W. Zhou, *J. Colloid Interface Sci.*, **533**, 24 (2019); https://doi.org/10.1016/j.jcis.2018.08.047
35. A.S. Kshirsagar, A. Gautam and P.K. Khanna, *J. Photochem. Photobiol. A: Chem.*, **349**, 73 (2017); https://doi.org/10.1016/j.jphotochem.2017.08.058
36. T. Dong, P. Wang and P. Yang, *Int. J. Hydrogen Energy*, **43**, 20607 (2018); https://doi.org/10.1016/j.ijhydene.2018.09.079
37. Z. Yue, A. Liu, C. Zhang, J. Huang, M. Zhu, Y. Du and P. Yang, *Appl. Catal. B: Environ.*, **201**, 202 (2017); https://doi.org/10.1016/j.apcatb.2016.08.028
38. M.M. Rhaman, S. Ganguli, S. Bera, S.B. Rawal and A.K. Chakraborty, *J. Water Process Eng.*, **36**, 101256 (2020); https://doi.org/10.1016/j.jwpe.2020.101256
39. J.T. Adeleke, T. Theivasanthi, M. Thiruppathi, M. Swaminathan, T. Akomolafe and A.B. Alabi, *Appl. Surf. Sci.*, **455**, 195 (2018); https://doi.org/10.1016/j.apsusc.2018.05.184
40. J. Cheng, Y. Shen, K. Chen, X. Wang, Y. Guo, X. Zhou and R. Bai, *Chin. J. Catal.*, **39**, 810 (2018); https://doi.org/10.1016/S1872-2067(17)63004-3
41. S.M. Aydoghmish, S.A. Hassanzadeh-Tabrizi and A. Saffar-Teluri, *Ceram. Int.*, **45**, 14934 (2019); https://doi.org/10.1016/j.ceramint.2019.04.229